ARCHIVES OF ELECTRICAL ENGINEERING VOL. 69(1), pp. 5–21 (2020)

DOI 10.24425/aee.2020.131755

Research on emergency DC power support coordinated control for hybrid multi-infeed HVDC system

CONGSHAN LI, YIKAI LI, JIAN GUO, PING HE

School of Electrical and Inf ormation Engineering, Zhengzhou University of Light Industry
Henan, no. 5 Dongfeng road Zhengzhou, China
e-mail: 1553614050@qq.com

(Received: 23.04.2019, revised: 22.07.2019)

Abstract: Based on the respective characteristics of line-commutated converter high-voltage direct current (LCC-HVDC) and voltage-source converter high voltage direct current (VSC-HVDC), two additional emergency DC power support (EDCPS) controllers are designed, respectively. In addition a coordinated control strategy based on a hybrid multi-infeed HVDC system for EDCPS is proposed. Considering the difference in system recovery between LCC-HVDC and VSC-HVDC in EDCPS, according to the magnitude of the amount of potential power loss, the LCC-HVDC and VSC-HVDC priority issues of boosting power for EDCPS are discussed in detail. Finally, a hybrid three-infeed HVDC that consists of two parallel LCC-HVDCs and one VSC-HVDC that is built in PSCAD/EMTDC are simulated. The effectiveness of the proposed approach is verified based on this hybrid three-infeed HVDC system.

Key words: additional controllers, coordinated control, EDCPS, hybrid multi-infeed HVDC system, HVDC

1. Introduction

Line-commutated converter based high voltage direct current (LCC-HVDC), especially in ultra-HVDC systems (UHVDC), is in an influential position in the electric energy transmission field due to its advantages of trans-regional, long-distance and bulk power. Because it uses the thyristor as the commutation device, there is only one control degree of freedom in the trigger delay angle, and a commutation failure easily occurs. It also consumes a large amount of reactive power during commutation, which accounts for 40–60% of the transmission power [1]. At present, a fully controlled power electronics device represented by the insulated gate bipolar transistor (IGBT) is favored in the field of high voltage direct current transmission, and it is named voltage-

source converter based high voltage direct current (VSC-HVDC). VSC-HVDC, based on the voltage source converter (VSC) and pulse width modulation (PWM), can realize fast decoupling control of active and reactive power and has excellent dynamic performance.

VSC-HVDC plays an important role in the global energy interconnection due to its flexible and controllable technical means. VSC-HVDC can realize the massive scale of wind-solar complementary power generation, as well as flexible interaction between clean energy and an energy storage system. The VSC-HVDC can solve the impact of indirect energy on the receiving-end power grid and is an indispensable brace for building a robust smart grid. Specifically, in May 2017, TBEA developed the world's first ultrahigh voltage (UHV) VSC-HVDC converter valve, which upgraded the voltage level of VSC-HVDC to the UHV level of ±800 kV, this was a milestone in the history of the development of VSC-HVDC [2].

With the large-scale access of clean energy to load centers, the future power grid will inevitably have multiple LCC-HVDC and VSC-HVDC feeds into the same or close electrical distance system, which ultimately form a hybrid multi-infeed HVDC. For example, a LCC-HVDC line is operated in the Shanghai Luchao port – Shengsi island, and one terminal of the Zhoushan five-terminal VSC-HVDC project is also located on Shengsi island [3], thus forming a parallel hybrid double-infeed HVDC system on Shengsi island. At present, the research on hybrid multi-infeed HVDC in domestic and foreign references are focuses mostly on the reactive power support ability of VSC-HVDC for an AC system to enhance the capacity of LCC-HVDC to suppress commutation failure, and the law of mutual interaction between LCC-HVDC and VSC-HVDC. Reference [4] proposed a novel coordinated control approach based on the reactive power compensation of modular multilevel converter high-voltage direct current (MMC-HVDC) to mitigate the commutation failure of LCC-HVDC in a hybrid multi-infeed HVDC system. Reference [5] proposed an efficient approach for commutation failure immunity level assessment based on the commutation failure immunity index in a hybrid multi-infeed HVDC system. Reference [6] presented the stability simulation results of two equivalent aggregated offshore wind farms based on a doubly-fed induction generator fed to two power grids through a hybrid multi-infeed HVDC system. Based on eigen-analysis, the impact of the Short-Circuit-Ratio (SCR) values of the LCC-HVDC and VSC-HVDC links, and the proximity between line-commutated converter (LCC) and VSC inverter stations on the dynamics of the hybrid multi-infeed HVDC system is investigated in reference [7], and then it is presented to systematically optimize the controller parameters for the hybrid multi-infeed HVDC system attached to a weak AC grid. The positive contribution of the MMC-HVDC link to the LCC-HVDC link in the area of the commutation failure immunity index (CFII), effective short circuit ratio (ESCR), voltage sensitivity factor (VSF), temporary overvoltage (TOV), and DC line fault recovery are investigated in reference [8] for the hybrid multi-infeed HVDC system. As far as EDCPS is concerned, there are also many references. When the AC grid is disturbed, the HVDC system can change the transmission power for rapid EDCPS and play a role in the controlling of frequency stability [9–10]. Reference [11] investigated constraint factors of EDCPS for HVDC systems. References [12, 13], and [14] points out that HVDC emergency control can significantly improve the transient stability of an AC/DC interconnected power grid. A prediction model of post-disturbance steady frequency is proposed in [15], which considers the EDCPS and the frequency response of AC grids on both sides of the HVDC link, aiming at the problem of frequency stability of the asynchronous AC/DC hybrid power grid.

The HVDC system has a large active power adjustment capability. If serious faults occur in an AC/DC hybrid or multi-infeed HVDC power transmission system, the short-time overload

capability of the normally operating DC system can be utilized. The DC power injected into the AC system is rapidly modulated to realize the EDCPS of the DC system to the AC system, which can compensate for the power imbalance of the sending-receiving ends in the transient process and improve the transient stability of the system. EDCPS has become an economically viable emergency control measure because of its fast, reliable and large adjustment capacity. Besides, the impact of tie line failure on the power system is greatest. Because once the tie line fails, the power of the sending-receiving ends will be seriously unbalanced. At this time, the EDCPS can play a good control effect and significantly improve the transient stability of the interconnected transmission system.

The references mention above hardly relate to the transient stability of a hybrid multi-infeed HVDC system under EDCPS. Therefore, this paper is based on the existing research on EDCPS, it studies the transient stability of a hybrid multi-infeed HVDC system under EDCPS. According to the control characteristics of LCC-HVDC and VSC-HVDC, additional EDCPS controllers have been designed. Aiming at the magnitude of the amount of potential power loss, a coordinated control strategy for power allocation of a hybrid multi-infeed HVDC system during EDCPS is proposed. The effectiveness of the control strategy is verified by simulation.

2. Electromagnetic transient model of hybrid multi-infeed HVDC

The hybrid three-infeed HVDC model is shown in Fig. 1. L in Fig. 1 refers to electrical distance. Specifically, if $L = 0$, the hybrid multi-infeed HVDC system feeds into the same AC system.

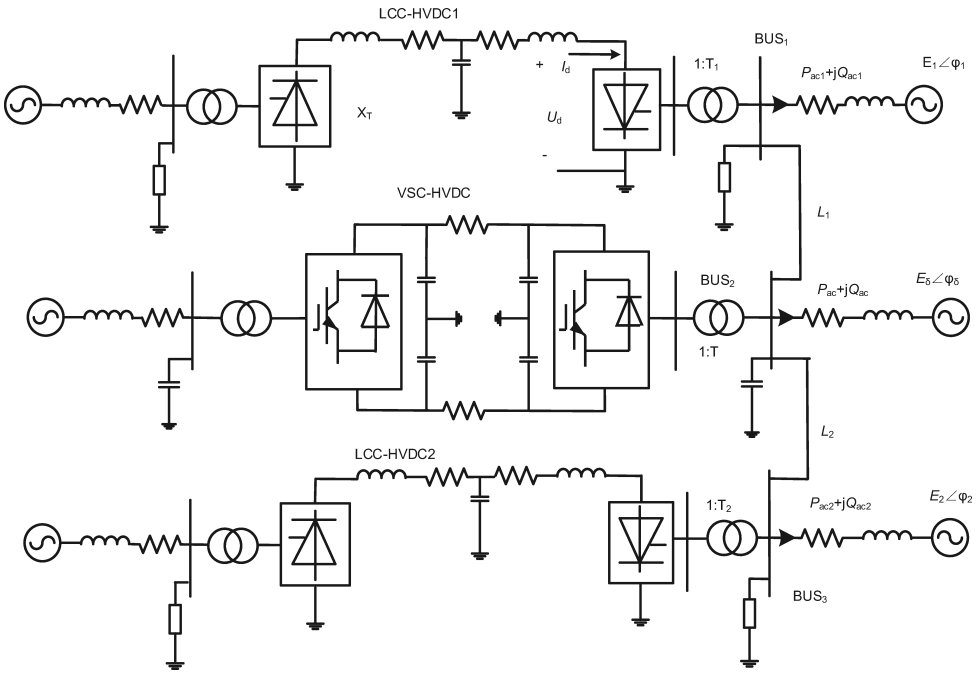

Fig. 1. Schematic diagram of hybrid there-infeed HVDC

Here, P_{ac} and Q_{ac} are the active and reactive power of the AC system of each subsystem, respectively; T_1, T and T_2 are the converter transformers ratios, respectively; X_T is the smoothing reactor; $E_1\angle\phi_1$, $E_\delta\angle\phi_\delta$, $E_2\angle\phi_2$ are the equivalent electromotive force and impedance of the AC system in each subsystem, respectively.

2.1. LCC-HVDC subsystem

The LCC-HVDC subsystem is modified from the International Council on Large Electric systems (CIGRE) standard test model. The rectifier is controlled by a constant current and minimum angle α. The inverter side is controlled by a constant current and angle γ. The primary system parameters are listed in Table 1.

Table 1. Main parameters of the LCC-HVDC

LCC-HVDC	Rectifier parameters	Inverter parameters
AC system	382.87 kV 47.7∠84°Ω	215.05 kV 21.2∠75°Ω
Reactive power compensation capacity	500 Mvar	500 Mvar
Converter transformer	600 MVA	590 MVA
Smoothing reactor	0.5968 H	0.5968 H

2.2. VSC-HVDC subsystem

To obtain high-quality current response, the VSC-HVDC subsystem employs the dual-closed loop structure of a current inner loop and voltage/power outer loop. The inner current loop controller adopts dq decoupling control. The underlying principle is that the three-phase current in the abc three-phase stationary coordinate system into the dq two-phase synchronous rotating coordinate system, then via controlling the d-axis or q-axis current to govern modulation degree and a phase angle of the converter, such that active and reactive power independent decoupling control is realized [16]. To avoid further deterioration of the AC bus voltage on the inverter and commutation failure of LCC-HVDC, a constant active power and constant reactive power control are adopted on the rectifier, and a constant DC voltage and constant AC voltage are utilized on the inverter [17]. The core block diagram of the VSC-HVDC control is shown in Fig. 2. The primary system parameters are shown in Table 2.

Table 2. Main parameters of the VSC-HVDC

VSC-HVDC	Rectifier parameters	Inverter parameters
AC system	445 kV 44.7∠84°Ω	215 kV 21.2∠75°Ω
Converter transformer	500 MW 420/170 kV	500 MW 230/165 kV
DC capacitance	300 μF	300 μF

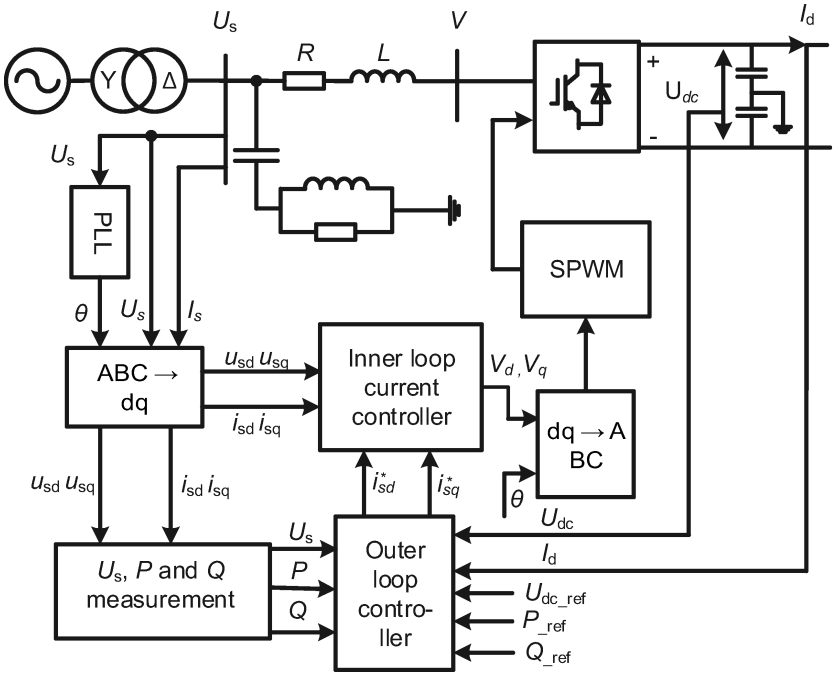

Fig. 2. VSC controller structure diagram

Here, PLL is the phase-locked loop, θ is the angle of power grid side voltage, U_s is the power grid side voltage, I_s is the power grid side current, V is the AC side voltage of converter, R is the equivalent loss of the system, and L is the commutation inductor. U_{sd}, U_{sq} are the components of U_s on the$d$-axis and the q-axis, i_{sd}, i_{sq} are the components of I_s on the d-axis and the q-axis; V_d, V_q are the components of V on the d-axis and the q-axis. i^*_{sd}, i^*_{sq} are the reference values of active current and reactive current; P, Q are the measured values of active power and reactive power; $P_{\_\mathrm{ref}}$, $Q_{\_\mathrm{ref}}$ are the reference values of active power and reactive power.

3. Analysis and research on EDCPS

3.1. EDCPS mechanism

The overload capacity of the LCC-HVDC system refers to the overload capacity of the thyristor, which is the magnitude and duration of the DC current above the rated value. The overload capacity of the thyristor can be divided into three cases: (a) long-term operation – the current value is less than 1.2 times the rated DC current; (b) short-term overload – generally choose 2 h for short-term overload time, it takes 1.1 times the rated DC current value; (c) temporary overload – the time is generally less than 5 s and the overload capacity can reach 1.3 times or even 1.5 times the rated DC current [18].

The overload capacity of the VSC-HVDC system is mainly limited by two conditions: i) the maximum current $I_{\max}$ is allowed to flow through the converter valve, and $I_{\max}$ determines the maximum power that is exchangeable between the inverter and the AC system; and ii) the maximum steady-state DC current $I_{dc\text{-}\max}$, which allows flow through the DC transmission line, and the $I_{dc\text{-}\max}$ determines the range of active power transmission.

The principle of EDCPS to improve the stability of the system has been described in many references. The core of this principle is to utilize the extended equal area criterion (EEAC) of the transient process under large disturbances to illustrate [18, 19]. The EEAC theory divides the system under severe faults into two-machine instability mode, which is divided into a severely disturbed groups (S groups) and a remnant groups (A groups). The stability problem of the overall system is the relative stability problem of the two groups. The transient equations of motion for the S groups and the A groups are as follows:

$$\begin{cases} \dot{\delta}_S = \omega_S \\ M_S\dot{\omega}_S = \sum\limits_{i\in S}(P_{mi} - P_{ei}) \\ M_S\delta_S = \sum\limits_{i\in S} M_i\delta_i \\ M_S\omega_S = \sum\limits_{i\in S} M_i\omega_i \\ M_S = \sum\limits_{i\in S} M_i \end{cases}, \tag{1}$$

$$\begin{cases} \dot{\delta}_S = \omega_A \\ M_A\dot{\omega}_A = \sum\limits_{i\in A}(P_{mj} - P_{ej}) \\ M_A\delta_A = \sum\limits_{i\in A} M_j\delta_j \\ M_A\omega_A = \sum\limits_{i\in A} M_j\omega_j \\ M_A = \sum\limits_{i\in A} M_j \end{cases}, \tag{2}$$

where M, δ and ω are the equivalent inertia time constant, the equivalent power angle and the equivalent angular frequency. The subscript S represents the S groups, A represents the A groups, and i and j are the i-th generators and the j-th generators, respectively. P_m is the equivalent mechanical power, P_e is the equivalent electromagnetic power. Equations (1) and (2) are merged into a single machine infinite bus system, from which one can obtain Equation (3):

$$\begin{cases} \delta_{SA}^{\&} = \omega_{SA} \\ \delta_{SA} = \delta_S - \delta_A \\ \omega_{SA} = \omega_S - \omega_A \\ \omega_{SA}^{\&} = \dfrac{1}{M_S}\sum\limits_{i\in S}(P_{mi} - P_{ei}) - \dfrac{1}{M_A}\sum\limits_{i\in S}(P_{mj} - P_{ej}) \end{cases}. \tag{3}$$

During normal operation of the HVDC system, if $\omega_{SA} = 0$, then the generator power angle is in a stable state. In the HVDC system, taking the three-phase short-circuit fault in the S groups as an example, the electromagnetic power in the S groups is less than the mechanical power, and the generator rotor will perform the acceleration motion. If the power of emergency support is equivalent to the electromagnetic power of the generator, and by adding the EDCPS measures to Equation (3), then Equation (3) becomes Equation (4). From Equation (4), after adding emergency power support measures, ω_{SA} tends to zero, so power angle stability can be achieved, where ΔP_e is the amount of EDCPS.

$$\begin{cases} \delta_{SA}^{\&} = \omega_{SA} \\ \omega_{SA} = \dfrac{1}{M_S}\displaystyle\sum_{i\in S}[P_{mi} - (P_{ei} + \Delta P_e)] - \dfrac{1}{M_A}\sum_{j\in A}\left[P_{mj} - (P_{ej} + \Delta P_e)\right] \\ \delta_{SA} = \delta_S - \delta_A \\ \omega_{SA}^{\&} = \omega_S - \omega_A \end{cases} . \tag{4}$$

3.2. LCC-HVDC and VSC-HVDC additional EDCPS controller design

EDCPS is a kind of DC large-mode modulation, which is one of the most economical and effective ways to maintain grid transient stability. The EDCPS control measures of LCC-HVDC and VSC-HVDC are different in restraining power angle swing and improving frequency stability. Therefore, two types of active additional controllers are designed in this paper, all of which are open loop control.

LCC-HVDC additional EDCPS controller design

Assuming that the system only contains the fundamental component, the simple mathematical model of the LCC-HVDC converter is as follows [20]:

$$\begin{cases} U_{d0} = \dfrac{3\sqrt{2}}{\pi}U_{ac} \\ U_d = U_{d0}\cos\gamma - \dfrac{3X_c}{\pi}I_d \\ I_d = \dfrac{U_{d0r}\cos\alpha - U_{d0i}\cos\beta}{R_{cr} + R_{ci} + R_L} \\ \varphi \approx \cos^{-1}\left(\dfrac{U_d}{U_{d0}}\right) \\ P_{ac} = P_{dc} = U_d I_d \\ Q_{ac} = Q_{dc} = P\tan\varphi \end{cases} , \tag{5}$$

where U_{d0} is the no-load DC voltage; U_{ac} is the AC voltage root mean square (RMS); U_d is the DC voltage; γ is the commutation extinction angle; I_d is the DC current; U_{d0r} and U_{d0i} are the no-load DC voltages on the rectifier side and the inverter side, respectively; R_{cr} and R_{ci} represent the commutation reactance of the rectifier side and inverter side, respectively; φ is the converter power factor angle; P_{ac} and P_{dc} are the AC power and DC power, respectively, and they are numerically equal when loss is neglected; α is the thyristor's trigger delay angle; β is the trigger advance angle.

It can be concluded from Equation (5) that boosting power by reducing γ to increase DC voltage is very limited during overload operation of the converter [20]. Hence, this paper chooses to add an EDCPS controller of LCC-HVDC on the constant current control module of the rectifier. And it can, via boosting the DC current, perform emergency power support on the basis of the principle of equal-amplitude step-by-step increments. The signal of the power support is shown in Fig. 3. Each time boost adds 20% of the amount of EDCPS. The EDCPS controller of LCC-HVDC is shown in Fig. 4. The current, voltage and power are all taken as the per-unit value.

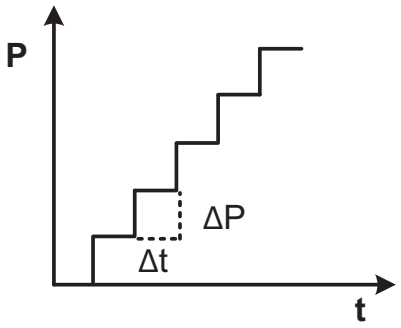

Fig. 3. Increasing block power

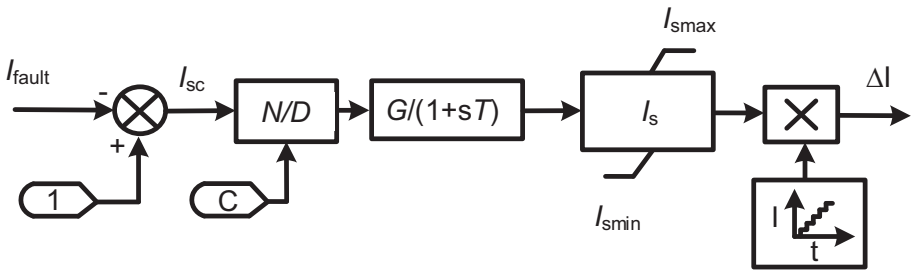

Fig. 4. EDCPS controller of the LCC-HVDC

In Fig. 4, I_{fault} is the current signal of the fault HVDC line, 1 minus I_{fault} gets the initial current support signal I_{sc}. C serves as a constant, and I_{sc} divided by C can get the support current signal I_s. The value of C can be 1 or $I_{sc}/0.5$, when C is 1, I_{sc} is the same as I_s, which indicates that LCC-HVDC operates within 1.5 times the overload range, and C is $I_{sc}/0.5$, which indicates that LCC-HVDC operates at a maximum 1.5 times overload. I_s multiplied by the step-by-step signal can obtain the additional controller output of the DC current incremental signal ΔI. While the system is in a steady-state, the incremental signal is zero, and the additional controller doesn't work. In the event of a fault, this signal is superimposed on the non-faulted LCC-HVDC rectifier constant current control module, and the trigger signal is sent to the valve control unit via the pole control stage to achieve EDCPS. To ensure unnecessary malfunction of the EDCPS controller, the limit link is set to ±5% of the normal transmission power.

VSC-HVDC additional EDCPS controller design

In this paper, the *dq* decoupling control method of double closed-loop structure is employed. The outer loop controller produces the current reference values of the *d*-axis and the *q*-axis. The inner loop controller implements tracking control of the current reference value and generates the required converter reference current [21]. The VSC mathematical model in the *dq* coordinate system is as follows:

$$\begin{cases} i_{sd}R + L\dfrac{\mathrm{d}i_{sd}}{\mathrm{d}t} = u_{sd} - V_d + \omega L i_{sq} \\ i_{sq}R + L\dfrac{\mathrm{d}i_{sq}}{\mathrm{d}t} = u_{sq} - V_q + \omega L i_{sd} \end{cases}. \tag{6}$$

According to the feed forward compensation decoupling control and instantaneous power calculation method [22], the grid voltage vector is orientated along the *d*-axis. Therefore, the grid voltage vector can be derived from Equation (7):

$$\begin{cases} P = 1.5 u_s i_{sd} \\ Q = -1.5 u_s i_{sq} \end{cases}. \tag{7}$$

Therefore, the active power can be controlled by controlling the *d*-axis current. In this paper, the additional EDCPS controller is designed based on the VSC-HVDC active power control loop, as shown in Fig. 5. The actual measures fault HVDC power signal is output to the modulation signal P_{mod} through the EDCPS link, and then P_{mod} is superimposed on the active command value of the active power control loop of the *d*-axis to achieve emergency power adjustment.

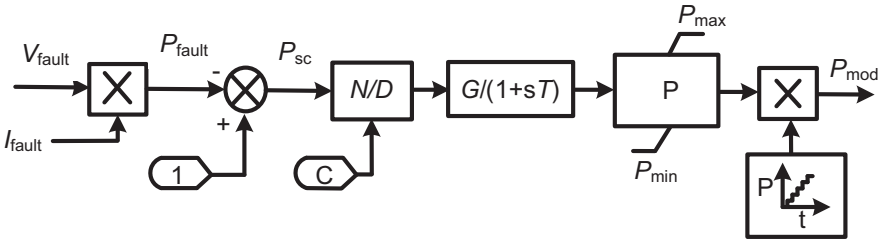

Fig. 5. EDCPS controller of VSC-HVDC

In Fig. 5, P_{fault} is a fault line active power signal, 1 minus P_{fault} gets the initial power support signal P_{sc}. C serves as a constant, and P_{sc} divided by C can get the power support signal P. The value of C can be 1 or $P_{sc}/0.5$. When C is 1, P_{sc} is the same as P, indicating that VSC-HVDC operates within 1.5 times the overload range. When C is $P_{sc}/0.5$, this indicates that VSC-HVDC operates at a maximum of 1.5 times the overload. P is multiplied by the step-by-step signal to obtain the additional controller output of the active power boost signal P_{mod}.

Additional controllers aim to improve the transient stability of the hybrid multi-infeed HVDC system by making full use of the fast regulation capability of normal operation HVDC after power vacancy occurs in the system. The power modulation of each HVDC is determined by its own control signal, which can operate independently without affecting the other. They can also cooperate with each other to improve the stability of the system and ensure that the magnitude of the power boost amount should be within the converter overload range.

4. Coordinated control strategy of EDCPS for LCC-HVDC and VSC-HVDC

EDCPS of the hybrid multi-infeed HVDC system relates to two core issues. One is how to design the additional EDCPS controllers to achieve smooth transfer of power. The other is the amount of power support allocation strategy, which means how to achieve the amount of power support allocated reasonably between LCC-HVDC and VSC-HVDC. The power allocation of EDCPS is essentially the impact of power flow transfer on the support effect, and unreasonable power allocation will bring adverse effects on the system.

Reference [23] studied the coordinated control strategy of LCC-HVDC and VSC-HVDC interconnection systems, the appropriate parameters and control dead zone can be set on the designed additional controller, so that the power support amount is distributed reasonably between the LCC-HVDC and VSC-HVDC. Reference [24] points out that different types of EDCPS have different effects on the transient stability of whole system. Therefore, there is a problem of power support priority of LCC-HVDC and VSC-HVDC. The emergency power support priority needs to be determined according to the power boost level when the power boost amount is relatively small (the LCC-HVDC rated DC power is 1000 MW in this paper, which was achieved by setting the power loss value and performing simulation experiments one by one; this paper is set to 15% of the maximum power loss amount when HVDC is blocked), which can preferentially boost the power of LCC-HVDC. If the system has a large power loss amount but doesn't exceed the maximum overload capacity of the HVDC system, it can preferentially boost the VSC-HVDC power. If priority is given to boost the LCC-HVDC power, then the LCC-HVDC will consume a large amount of reactive power and the reactive power is insufficient, which results in the power being unable to increase to the command value. If boosting the power of LCC-HVDC or VSC-HVDC alone cannot make the system stable, it is necessary to consider the LCC-HVDC and VSC-HVDC participation in EDCPS. In addition, if the VSC-HVDC itself fails, if there are other VSC-HVDCS in the system, the power of the VSC-HVDC system will be boosted preferentially, otherwise the power of the LCC-HVDC system will be boosted. Considering that the boost power of LCC-HVDC will consume more reactive power, it is necessary to configure reactive power compensation. The compensation capacity is equipped according to 50% of the HVDC full load operation.

In this paper, the load model is based on a polynomial model, and considering the static load model of the frequency term [25], the load power is calculated by Equation (8):

$$\begin{cases} P_L = P_0 \left[P_Z \left(\dfrac{U}{U_0} \right)^2 + P_I \left(\dfrac{U}{U_0} \right) + P_P \right] \left(1 + K_{DP} \dfrac{f - f_0}{f} \right) \\ Q_L = Q_0 \left[Q_Z \left(\dfrac{U}{U_0} \right)^2 + Q_I \left(\dfrac{U}{U_0} \right) + Q_P \right] \left(1 + K_{DQ} \dfrac{f - f_0}{f} \right) \end{cases}, \tag{8}$$

where P_Z is the active power proportional coefficient of the constant impedance term, P_I is the active power proportional coefficient of the constant current term, P_P is the active power proportional coefficient of constant power term, and Q_Z, Q_I, and Q_P are the reactive power

proportional coefficients, then

$$\begin{cases} P_Z + P_I + P_P = 1 \\ Q_Z + Q_I + Q_P = 1 \\ K_{DP} = 1 \\ K_{DQ} = -1 \end{cases}, \tag{9}$$

where K_{DP} and K_{DQ} are the load frequency factor, which is the coefficient of load power as a function of frequency, U is the current voltage value, and U_0 is the initial voltage value.

Ignoring the system loss and supposing no rotating reserve in this paper, the following factors are considered: primary frequency regulation of generator P_{pf} and load frequency control ΔP_L, and K_G, which is the unit generator regulation of power. Assuming that the active power loss amount of the system after the HVDC fault is set to the balanced power P_{balance}, the amount of EDCPS demanded in the system is as follows:

$$\begin{cases} P = P_{\text{balance}} - P_{pf} - \Delta P_L \\ P_{pf} = K_G\,(f - f_0) \end{cases}. \tag{10}$$

According to the modulation priority and power support amount set above, the following coordinated control strategy is as follows:

1. The power loss amount is lower than the threshold, and the amount P_{LCC} of power is preferentially boosted for EDCPS, and the power support amount P_{LCC} is calculated according to Equation (10).
2. If the power loss amount exceeds the threshold, the VSC-HVDC is preferentially boosted for EDCPS, and the P_{VSC} is calculated according to equation (10).
3. If the amount of power loss exceeds the maximum overload capacity of VSC-HVDC, the LCC-HVDC requires joint participation to maintain the system stability. The amount of LCC-HVDC participation in the emergency power support is as follows:

$$\Delta P_{\text{LCC}} = P - \Delta P_{\text{VSC}}, \tag{11}$$

   where P_{LCC} pertains to the amount of LCC-HVDC power support, and P_{VSC} pertains to the amount of VSC-HVDC power support amount.
4. If the total EDCPS of VSC-HVDC and LCC-HVDC is unable to restore system stability, then generator tripping or load shedding is required:

$$P_{\text{shed}} = P - \Delta P_{\text{LCC}} - \Delta P_{\text{VSC}}. \tag{12}$$

5. Simulations

To verify the EDCPS scheme in this paper, an electromagnetic transient model based on PSCAD/EMTDC is established as shown in Fig. 1. The following simulation studies are performed based on this model: (a) verification of EDCPS for LCC-HVDC additional control; (b) verification of EDCPS for VSC-HVDC additional control; (c) verification of EDCPS for LCC-HVDC and VSC-HVDC coordinated control. Furthermore, to inhibit commutation failure due to fast DC power elevation, the elevating rate is set to 4–5 pu/s after several simulation experiments.

5.1. Verification of EDCPS for LCC-HVDC additional control

The LCC-HVDC1 was set to reduce the transmission capacity by 150 MW at 4 s, and it was set to clear the fault at 6 s. Because the amount of power loss doesn't exceed the threshold, so LCC-HVDC or VSC-HVDC can be selected for EDCPS. The major operating state of the system with the same power support of VSC-HVDC is compared. The simulation results are presented in Fig. 6.

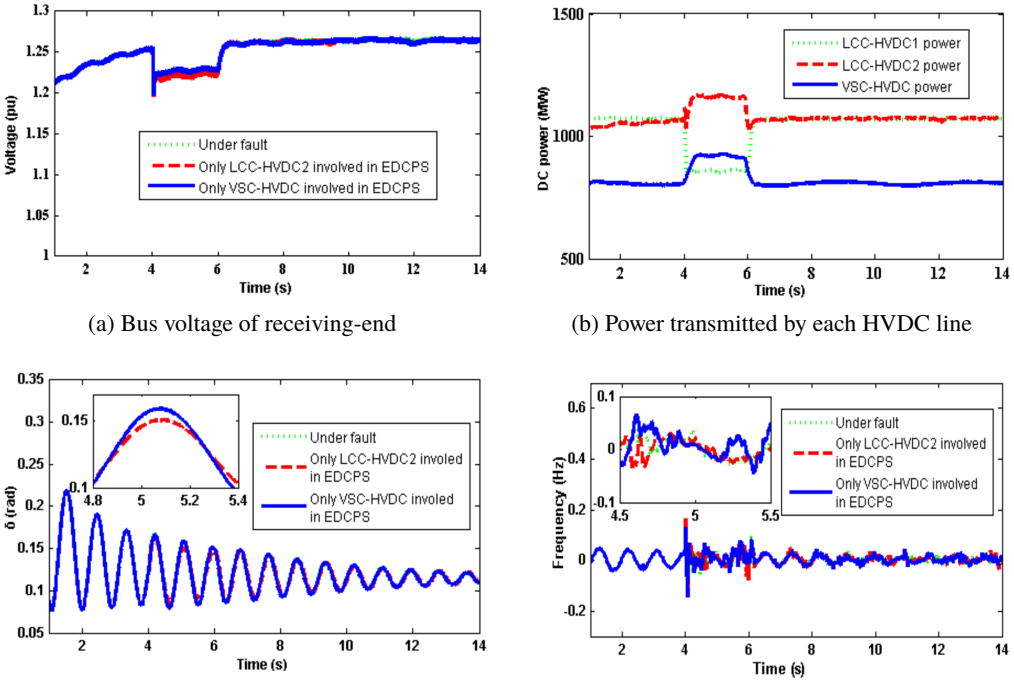

(a) Bus voltage of receiving-end

(b) Power transmitted by each HVDC line

(c) VSC-HVDC inverter generator power angle

(d) Frequency difference on sending-receiving end of system

Fig. 6. Simulation results of EDCPS controller for LCC-HVDC

Fig. 6 shows a comparative analysis of simulation waveforms with the choice of LCC-HVDC power support versus VSC-HVDC power support. Fig. 6(a) shows that when the amount of system power doesn't exceed 15%, the receiving-end bus voltage declines by 0.05 pu, namely the voltage fluctuation of the AC bus on the inverter side is small. The load power and primary frequency regulation variations can also be derived from the simulation, which is not shown here. The same is true for case 5.2 and case 5.3. As it can be seen from Fig. 6(b) the LCC-HVDC2 is performed for EDCPS. As shown by Figs. 6(c) and (d), in the case of fault, the maximum variation of power angle is 0.03 pu and the maximum offset of frequency is 0.15 Hz, when the amount of system power loss is relatively small, it doesn't cause a large deviation in the power angle and frequency of the system. When LCC-HVDC2 is performed for EDCPS, the maximum power angle fluctuation is reduced by 0.01 pu compared to the fault. When the VSC-HVDC is employed for EDCPS, the power angle is almost unchanged compared with that of the fault. Thus, giving priority to boost

the LCC-HVDC power is better than the VSC-HVDC power in suppressing the power angle of generators and frequency fluctuation. Therefore, when the amount of the power loss of the system doesn't exceed the threshold, priority is given to boosting LCC-HVDC power.

5.2. Verification of EDCPS for VSC-HVDC additional control

The LCC-HVDC1 is set to reduce the transmission capacity by 500 MW at 4 s, and it was set to clear the fault at 6 s. During this time, the amount of power that the system needs to support exceeds 15% but doesn't exceed the maximum overload capacity of the HVDC system. Therefore, this paper chooses VSC-HVDC for EDCPS. The main operating state of the system when the LCC-HVDC boosts the same power is compared. The simulation results are shown in Fig. 7.

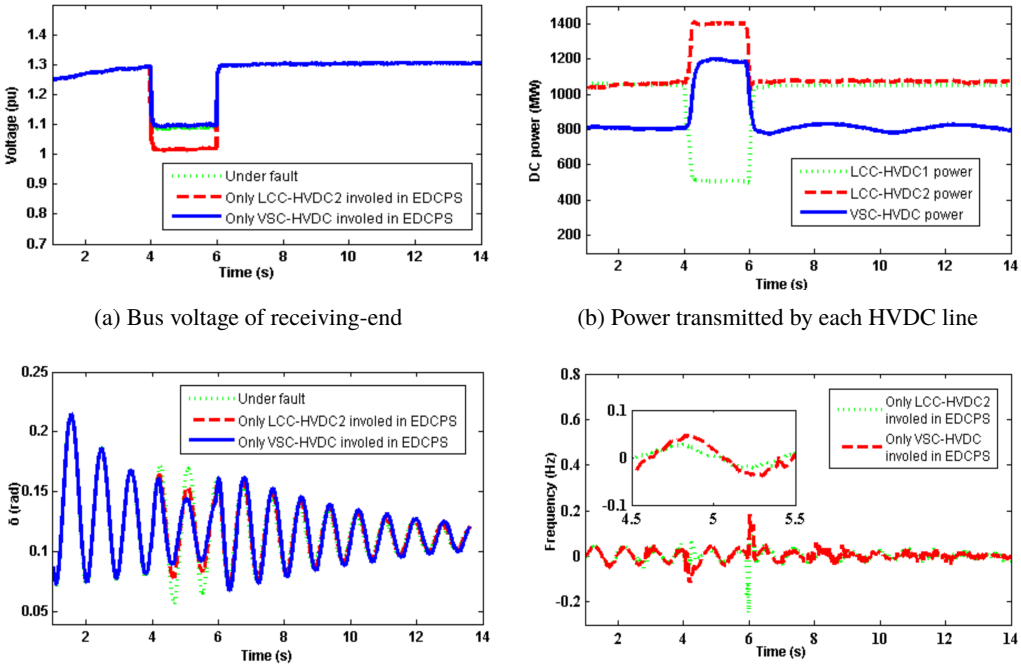

(a) Bus voltage of receiving-end

(b) Power transmitted by each HVDC line

(c) VSC-HVDC inverter generator power angle

(d) Frequency difference on sending-receiving end of system

Fig. 7. Simulation results of EDCPS controller for VSC-HVDC

To verify the priority of VSC-HVDC support in this case, Fig. 7 shows a comparative analysis of the simulation results for choosing LCC-HVDC power support versus VSC-HVDC power support. Fig. 7(a) shows that when the amount of system power loss exceeds 15%, the amount of power loss in this paper is 500 MW, at this time, the receiving-end bus voltage is reduced by 0.18 pu. When the LCC-HVDC is selected to perform EDCPS, the bus voltage drops by 0.26 pu, while the VSC-HVDC is performed EDCPS, the bus voltage is basically the same as the fault. Thus Fig. 7(a) shows that compared with the LCC-HVDC, if the amount of EDCPS exceeds 15%, then the power of the VSC-HVDC can be preferentially boosted to reduce the

impact on the bus voltage. For a more intuitive display LCC-HVDC power support versus VSC-HVDC power support, Fig. 7(b) shows the DC power of each HVDC system. Fig. 7(c) shows the generator power angle variation curve on the VSC-HVDC inverter side, as shown by Fig. 7(c) the maximum variation of power angle is 0.07 pu in the case of fault. When VSC-HVDC is performed for EDCPS, the maximum power angle fluctuation is reduced by 0.05 pu compared to the fault. And the LCC-HVDC2 is employed for EDCPS, the power angle is reduced by 0.04 pu compared to the fault. Both emergency power support approaches can diminish generator power angle oscillation, but from the simulation curve, the effect of VSC-HVDC power support is better than the effect of LCC-HVDC power support. Fig. 7(d) shows the frequency difference curve for sending-receiving ends of the overall system. From Fig. 7(d), it can be observed that the maximum offset of frequency is 0.20 Hz, when the amount of system power loss is relatively large, it fails to cause a large deviation in frequency of the system.

5.3. Verification of EDCPS for LCC-HVDC and VSC-HVDC additional control

The LCC-HVDC1 was set to DC that blocked the fault at 4 s and clear the fault at 6 s. Between 4 s – 6 s, DC power transmitted by LCC-HVDC1 is 0 WM. In this period of time, the power required to be supported exceeds the overload capacity of the HVDC system, and the amount of power support is greater than in cases 1 and 2. LCC-HVDC and VSC-HVDC coordinated control must be adopted to participate in the EDCPS. Fig. 8 shows the simulation results under LCC-HVDC and VSC-HVDC coordinated control.

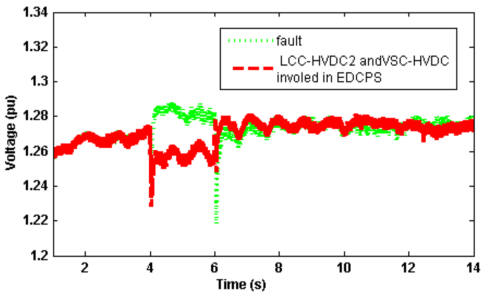

(a) Bus voltage of receiving-end

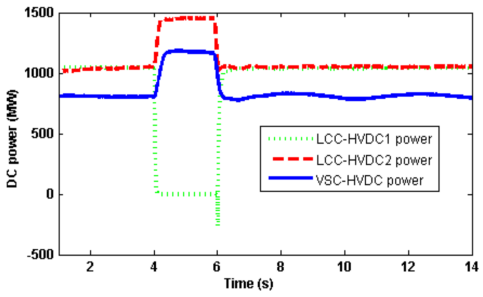

(b) Power transmitted by each HVDC line

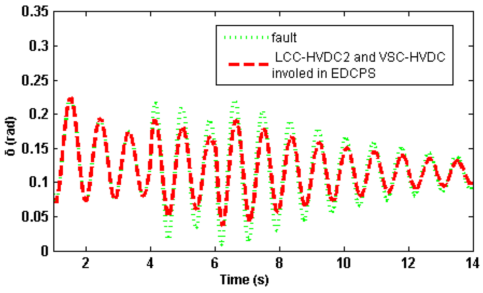

(c) VSC-HVDC inverter generator power angle

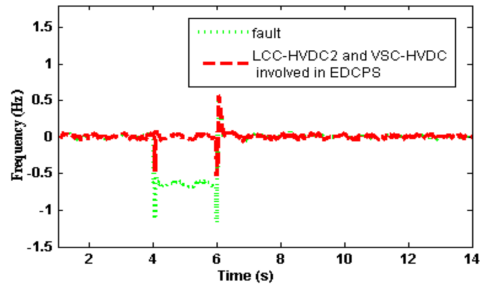

(d) Frequency difference on sending-receiving end of system

Fig. 8. Simulation results of LCC-HVDC and VSC-HVDC additional control

From Fig. 8(a), it can be observed that the reactive power has a large surplus during the LCC-HVDC1 blocking fault, since its DC blocking fault leads to the reduction of reactive power consumption, which causes the bus voltage of the receiving-end to rise. The amount of power for emergency support is 935 MW and exceeds the overload capacity of a single HVDC during the LCC-HVDC1 blocking fault. As shown in Fig. 8(b), the LCC-HVDC2 emergency boosts 500 MW and VSC-HVDC emergency boosts 435 MW to compensate for the power loss. Taking the power angle of the VSC inverter generator as an example, the maximum variation of power angle is 0.18 pu in the case of fault, Fig. 8(c) indicates that the generator power angle has a large amplitude oscillation during the fault period. After adopting coordinated control, the generator power angle oscillation amplitude is reduced, and the generator power angle can quickly and smoothly go to a stable state. From Fig. 8(d), it can be observed that the maximum offset of frequency is 0.65 Hz, which give rise to frequency collapse of the system. When the VSC-HVDC and the LCC-HVDC2 are jointly performed for EDCPS, the frequency fluctuation is maintained at around 0.05 Hz. Therefore, Fig. 8(d) also shows that the LCC-HVDC and VSC-HVDC coordinated control can reduce the frequency difference on sending-receiving ends of the system during the fault.

The above analysis shows that under this coordinated control, VSC-HVDC and LCC-HVDC can maximize the use of their overload capacity to bear the transmission power of the fault line and return to normal operation after fault clearance. The coordinated control plays a positive role in suppressing generator power angle oscillation and improving the bus frequency of the converter station.

6. Conclusions

The practical problems of energy distribution and load demand in China determine that HVDC is a significant means to achieve large-scale optimal energy allocation, and the hybrid multi-infeed HVDC system is the inevitable form of the future grid. In this paper, the research on EDCPS for the hybrid multi-infeed HVDC system is carried out, and the valuable conclusions are as follows:

1. Based on the DC power modulation function, the power emergency control is attached to the LCC-HVDC rectifier to realize independent and coordinated control of the transmission power of the nonfault HVDC system. Compared with the traditional ramp-type power boosting mode, the stepped boosting power can give an inverter a large extinction angle margin and reduce the probability of commutation failure.
2. Based on the characteristics of independent decoupling control of VSC-HVDC, an additional controller of the d-axis is designed to increase the active reference current of the d-axis, which is superimposed on the original active reference current to boost the active power in the emergency state and suppress the system oscillation. The VSC-HVDC can dynamically adjust the reactive power, which allows it to recover faster than the LCC-HVDC in the transient process. The VSC-HVDC can also provide reactive power support to the inverter's AC bus voltage to reduce the probability of LCC-HVDC commutation failure.

3. According to the characteristics of VSC-HVDC and LCC-HVDC, a power allocation strategy is proposed. In accordance with the established strategy, the amount of power support that needs to be boosted is allocated, which can maximize the DC power transmission capability of the HVDC system.

References

[1] Bahrman M.P., Johnson B.K., *The ABCs of HVDC Transmission Technologies*, IEEE Power and Energy Magazine, vol. 5, no. 2, pp. 32–44 (2007).

[2] Zhang Wei, *TBEA successfully developed the world's first VSC-UHVDC converter*, China Equipment Engineering, vol. 12, no. 6 (2017).

[3] Guo Chunyi, Liu Wei, Zhao Jian *et al.*, *Impact of control system on small-signal stability of hybrid multi-infeed HVDC system*, IET Generation, Transmission and Distribution, vol. 12, no. 19, pp. 4233–4239 (2018).

[4] Guo Chunyi, Zhizhong Yang, Ning Linru *et al.*, *A Novel Coordinated Control Approach for Commutation Failure Mitigation in Hybrid Parallel-HVDC System with MMC-HVDC and LCC-HVDC*, Electric Power Components and Systems, vol. 45, no. 16, pp. 1773–1782 (2017).

[5] Hao Xiao, Li Yinhong, Duan Xianzhong, *Efficient approach for commutation failure immunity level assessment in hybrid multi-infeed HVDC systems*, The Journal of Engineering, vol. 2017, no. 13, pp. 719–723 (2017).

[6] Li Wang, Yang Zhihao, Lu Xiuyu, Prokhorov A.V., *Stability Analysis of a Hybrid Multi-Infeed HVdc System Connected Between Two Offshore Wind Farms and Two Power Grids*, IEEE Transactions on Industry Applications, vol. 53, no. 3, pp. 1824–1833 (2017).

[7] Guo Chunyi, Liu Wei, Zhao Chengyong *et al.*, *Small-signal dynamics and control parameters optimization of hybrid multi-infeed HVDC system*, International Journal of Electrical Power and Energy Systems, vol. 98, pp. 409–418 (2018).

[8] Guo Qinglei, Yoon Minhan, Kim Chanki *et al.*, *Commutation failure and voltage sensitivity analysis in a hybrid multi-infeed HVDC system containing modular multilevel converter*, International Transaction on Electrical Energy System, vol. 26, no. 10, pp. 175–182 (2016).

[9] Li Hucheng, Yuan Yubo, Zhang Xiaoyi *et al.*, *Analysis of frequency emergency control characteristics of UHV AC/DC large receiving end power grid*, The Journal of Engineering, vol. 2017, no. 13, pp. 686–690 (2017).

[10] Wen Yunfeng, Chung C.Y., Ye Xi, *Enhancing Frequency Stability of Asynchronous Grids Interconnected with HVDC Links*, IEEE Transactions on Power Systems, vol. 33, no. 2, pp. 1800−1810 (2018).

[11] Weng H., Xu Z., Xu F., *Research on constraint factor of emergency power support of HVDC systems*, Proceedings of the CSEE, vol. 34, vol. 10, pp. 1519–1527 (2014).

[12] Li Congshan, He Ping, Wang Youy *et al.*, *HVDC Auxiliary Emergency Power Control Strategy for Power Disturbance in Two Different Positions of AC/DC Interconnection System*, Archives of Electrical Engineering, vol. 62, no. 2, pp. 245–263 (2019).

[13] Liu Chongru, Zhao Yunhao, Li Zengyin *et al.*, *Design of LCC HVDC wide-area emergency power support control based on adaptive dynamic surface control*, IET Generation, Transmission and Distribution, vol. 11, no. 13, pp. 3236–3245 (2017).

[14] Sanz I.M., Judge P.D., Spallarossa C.D. *et al.*, *Dynamic Overload Capability of VSC HVDC Interconnections for Frequency Support*, IEEE Transactions on Energy Conversion, vol. 32, no. 4, pp. 1544–1553 (2017).

[15] Hu Yi, Wang Xiaoru, Chen Dalin *et al.*, *Frequency stability control method considering limited EDCPS*, The Journal of Engineering, vol. 2019, no. 16, pp. 2698–2705 (2019).

[16] Chunyi Guo, Yi Zhang *et al.*, *Analysis of Dual-Infeed HVDC with LCC-HVDC and VSC-HVDC*, IEEE Transaction on Power Delivery, vol. 27, no. 3, pp. 1529–1537 (2012).

[17] Zhao Chengyong, Sun Ying, Li Guangkai, *Control strategy of VSC-HVDC in dual-infeed HVDC systems*, Proceedings of the CSEE, vol. 28, no. 7, pp. 97–103 (2008).

[18] Rui Zhao, Yingmin Zhang, Xingyuan Li *et al.*, *The Research on the Emergency DC Power Support Strategies of Deyang-Baoji HVDC Project*, IEEE Asia-Pacific Power and Energy Engineering Conference, Wuhan, China (2011).

[19] Huifan Xie, Yao Zhang, Chengjun Xia *et al.*, *Influence of load model on UHVDC Emergency DC Power Support strategy*, IEEE 3th International Conference on Electric Utility Deregulation and Restructuring and Power Techologies, Nanjing, China (2008).

[20] Jos Arrillaga, *High Voltage Direct Current Transmission*, Printed in England by Srort Runpress Ltd. (1998)

[21] Latorre H.F., Ghandhari M., Söder L., *Active and reactive power control of a VSC-HVDC*, Electric Power Systems Research, vol. 78, no. 10, pp. 1756–1763 (2007).

[22] Rodrguez P., Pou J. *et al.*, *Decoupled double synchronous reference frame PLL for power converters control*, IEEE Transactions Power Electronics, vol. 22, no. 2, pp. 584–592 (2007).

[23] Wang Xi, Li Xingyuan, Wei Wei, Ding Lijie, *Coordinated control strategy for interconnected transmission system of VSC-HVDC and LCC-HVDC*, Electric Power Automation Equipment, vol. 36, no. 12, pp. 102–108 (2016).

[24] Chen R., Sun Z., Yang Y. *et al.*, *Emergency Power Support Control Strategy of VSC-HVDC and LCC-HVDC Coordination*, Power Engineering Technology, vol. 36, no. 6, pp. 14–19 (2017).

[25] Yan Liu, Zhe Chen, *A Flexible Power Control Method of VSC-HVDC Link for the Enhancement of Effective Short-Circuit Ratio in a Hybrid Multi-Infeed HVDC System*, IEEE Transactions on Power Systems, vol. 28, no. 2, pp. 1568–1581 (2013).